Biometals (2009) 22:817–826
DOI 10.1007/s10534-009-9228-1

# Important roles of the conserved linker-KKS in human neuronal growth inhibitory factor

**Zhi-Chun Ding · Xin-Chen Teng · Qi Zheng · Feng-Yun Ni · Bin Cai · Yang Wang · Guo-Ming Zhou · Hong-Zhe Sun · Xiang-Shi Tan · Zhong-Xian Huang**

Received: 19 February 2009 / Accepted: 10 March 2009 / Published online: 21 March 2009


**Abstract** Metallothinein-3 (MT3), also named neuronal growth inhibitory factor (GIF), is attractive by its distinct neuronal growth inhibitory activity, which is not shared by other MT isoforms. The polypeptide chain of GIF is folded into two individual domains, which are connected by a highly conserved linker, KKS. In order to figure out the significance of the conserved segment, we constructed several mutants of human GIF (hGIF), including the K31/32A mutant, the K31/32E mutant and the KKS-SP mutant by site-directed mutagenesis. pH titration and DTNB reaction exhibited that all the three mutations made the $\beta$-domain lower in stability and looser. More significantly, change of KKS to SP also altered the general backbone conformation and metal–thiolate cluster geometry. Notably, bioassay results showed that the bioactivity of the K31/32A mutant and the K31/32E mutant decreased obviously, while the KKS-SP mutant lost inhibitory activity completely. Based on these results, we proposed that the KKS linker was a crucial factor in modulating the stability and the solvent accessibility of the $Cd_3S_9$ cluster in the $\beta$-domain through domain–domain interactions, thus was indispensable to the biological activity of hGIF.

**Keywords** Metallothionein · Neuronal growth inhibitory factor · Linker · Mutation · Cell culture

**Abbreviations**

| | |
|---|---|
| MT | Metallothionein |
| GIF | Growth inhibitory factor |
| AD | Alzheimer's disease |
| PD | Parkinson's disease |
| CNS | Central nervous system |
| cDNA | Complimentary DNA |
| IPTG | Isopropyl $\beta$-D-thiogalactoside |
| DTNB | 5,5′-Dithiobis-(1-nitrobenzoic acid) |
| PCR | Polymerase chain reaction |
| DTT | Dithithreitol |
| ESI-MS | Electrospray ionization mass spectrometry |
| PSI | Pounds per square inch |
| UV-vis | Ultraviolet-visible |
| CD | Circular dichroism |
| LMCT | Ligand-to-metal charge transfer |

Z.-C. Ding · X.-C. Teng · Q. Zheng · F.-Y. Ni · B. Cai · X.-S. Tan · Z.-X. Huang (✉)
Chemical Biology Laboratory, Department of Chemistry, Fudan University, 220 Han-Dan Road, 200433 Shanghai, China
e-mail: zxhuang@fudan.edu.cn

Z.-C. Ding
e-mail: 051022004@fudan.edu.cn

Y. Wang · G.-M. Zhou
Department of Anatomy, Histology and Embryology, Medical School, Fudan University, 200032 Shanghai, China

H.-Z. Sun
Department of Chemistry, The University of Hong Kong, Pokfulam Road, Hong Kong, China

| | |
|---|---|
| NMR | Nuclear magnetic resonance |
| MTT | 3-(4,5)-dimethylthiahiazo (-2-y1)-2,5-di-phenytetrazolium bromide |
| DMSO | Dimethyl sulfoxide |

## Introduction

Essential transition metal ions, such as copper and zinc, play important roles in neurobiology (Cai et al. 2005). Dysregulated metal metabolism occurs in many neurodegenerative disorders, such as Alzheimer's disease (AD; Adlard and Bush 2006), Parkinson's disease (PD; Rasia et al. 2005) and prion disease (Brown and Kozlowski 2004) etc. Brain has a regulatory network to achieve metal ions homeostasis. One component of this network is the protein family called metallothioneins (MTs; Kagi and Schaffer 1988; Margoshes and Vallee 1957).

Metallothioneins are small (~7 kDa), cysteine-rich proteins that bind both essential ($Zn^{2+}$, $Cu^{+}$) and toxic ($Cd^{2+}$, $Hg^{2+}$) metal ions (Kagi and Schaffer 1988). Four mammalian MT isoforms (MT1, MT2, MT3 and MT4) have been identified since its discovery. The third isoform, MT3, also named neuronal growth inhibitory factor (GIF), is mainly expressed in the central nervous system (CNS) and possesses neuronal growth inhibitory properties in vitro that distinguish it from the MT1 and MT2 isoforms (Palmiter et al. 1992; Uchida et al. 1991; Uchida and Tomonaga 1989). As a member of MT family, the amino acid sequence of GIF exhibits about 70% identity with those of MT1/2, including the preserved array of 20 cysteine residues. However, there are two inserts in GIF compared to MT1/2: a threonine (Thr) at position 5 and a glutamate-rich peptide near the C-terminus. In addition, all known GIF sequences contain the conserved $^{6}$CPCP$^{9}$ motif which is absent in all other members of MT family (Fig. 1).

Mutational studies have demonstrated that mutation of the unique $^{6}$CPCP$^{9}$ motif either to $^{6}$CSCA$^{9}$ or $^{6}$CTCT$^{9}$ abolishes the bioactivity of GIF (Hasler et al. 2000; Romero-Isart et al. 2002). The results of our simulation clearly showed that the $^{6}$CPCP$^{9}$ motif in the $\beta$-domain would induce constraints on the human GIF (hGIF) peptide chain and make the N-terminus (residue 1–13 of hGIF) form a particular conformation with two parallel proline residues (Ni et al. 2007). It is believed that such a conformation would function as "a rigid arm providing an interacting surface for protein–protein interactions" (Williamson 1994). The hydroxyl group of Thr5 is also pivotal to perform the bioactivity of GIF (Cai et al. 2006; Romero-Isart et al. 2002).

Since the discovery of GIF in human brain, the gene has been cloned from many mammalian species and the encoded proteins have also been isolated and studied extensively (Chung et al. 2002a; Kobayashi et al. 1993; Palmiter et al. 1992; Pountney et al. 1994; Uchida et al. 1991). However, till now, the structure

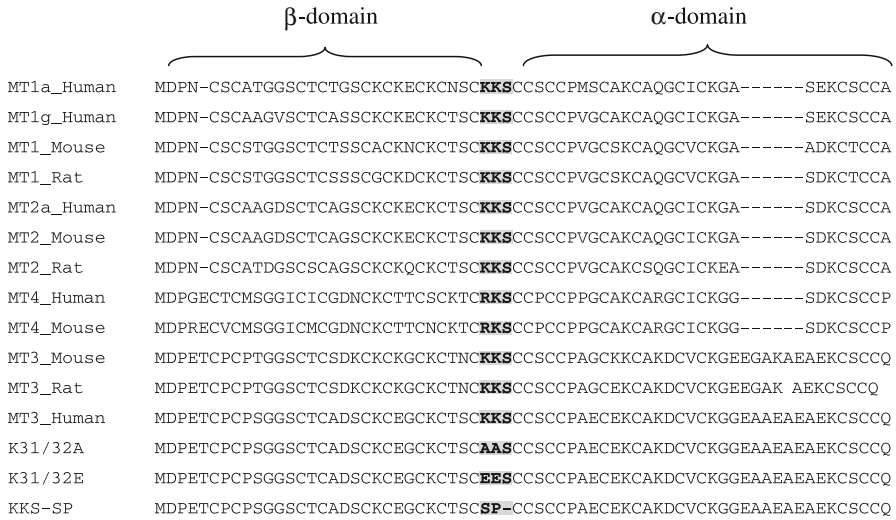


**Fig. 1** Amino acid sequences of mammalian metallothioneins. Polypeptides of all mammalian MTs are folded into two separate domains: the N-terminal $\beta$-domain and C-terminal $\alpha$-domain. The *black parts* indicate linker sequences

of the intact GIF molecule has not been determined by NMR or X-ray diffraction due to the highly dynamic properties of GIF, especially the $\beta$-domain (Faller et al. 1999; Oz et al. 2001; Wang et al. 2006). The spectroscopic characterization revealed that the polypeptide of GIF, like those of recombinant MT1/2, is folded into two domains connected by a short linker and binds seven bivalent metal ions. These metal ions are organized into two individual clusters: a distorted chair three-metal cluster, $M^{II}{}_3S_9$, in the N-terminal $\beta$-domain; and an adamantane-like four-metal cluster, $M^{II}{}_4S_{11}$, in the C-terminal $\alpha$-domain (Faller and Vasak 1997; Hasler et al. 1998).

Interestingly, the linker between the two domains is so conserved that it exists as a Lys-Lys-Ser (KKS) segment (Fig. 1) in all mammalian metallothioneins (except MT4, in which the conservative substitution linker RKS appears), which promotes us to explore the possible roles of the conserved linker sequence in structure and function of MTs. In order to figure out the role of the two positively charged lysine residues in neuronal growth inhibitory function of hGIF, we changed these two residues to uncharged residue Ala (the K31/32A mutant) and negatively charged residue Glu (the K31/32E mutant), respectively. In the crustacean MTs, the linker usually exists as XP (X stands for S, A or P) (Narula et al. 1995). In order to find out the functional difference between these two sequences, we changed KKS to SP (the KKS-SP mutant). Then UV-vis spectroscopy, CD spectroscopy, pH titration and DTNB reaction were employed to examine their structure and property differences. Finally, the inhibitory activities of hGIF and its variants were measured by rat neuronal cultures.

## Materials and methods

### Reagents

Fusion expression vector pGEX-4T-2, *Escherichia coli* strain *BL21*, glutathione Sepharose 4B, Superdex-75 and Sephadex G-25 were purchased from Phamacia Biotech (Uppsala, Sweden). T4 DNA ligase, dNTP and restriction enzymes (*Bam*HI and *Eco*RI) were purchased from New England Biolabs (Ipswich, MA, USA). Pfu DNA polymerase, cell culture reagents, isopropyl $\beta$-D-thiogalactoside (IPTG) and Triton-100 were purchased from Sangon (Shanghai, China). 2, 2′-dithiodipyridine, 5, 5′-Dithiobis-(1-nitrobenzoic acid) (DTNB), bovine thrombin (Catalog No. T4265) and 3-(4,5-dimethylthiahiazo-2-y1)-3,5-di-phenytetrazolium bromide (MTT) were from Sigma (St. Louis, MO, USA). Neurobasal-A medium and B27 serum-free supplements were purchased from GIBCO-BRL (Gaithersburg, MD, USA). The other reagents were of analytical grade.

### Cloning, expression and purification of hGIF and its variants

The hGIF gene was obtained by reverse transcription followed by polymerase chain reaction (PCR). The genes of the three mutants were constructed by PCR mutagenesis. Then, each PCR product was digested with *Bam*HI and *Eco*RI restriction enzymes and cloned into vector pGEX-4T-2.

Expression and purification of hGIF and its mutants were carried out as previously described (Yu et al. 2002). The final products were desalted, lyophilized and stored at −80°C.

### Protein reconstitution and characterization

The apo- and fully $Cd^{2+}$- or $Zn^{2+}$-loaded hGIF and its mutants were generated as previously described (Vasak 1991). The metal-to-protein ratios were determined by measuring the protein concentration via photometric sulphydryl groups (CysSH) quantification upon reaction with 2,2′-dithiodypridine in 0.2 M sodium acetate, 1 mM EDTA (pH 4.0), using an $\varepsilon_{343} = 7{,}600\ M^{-1}\ cm^{-1}$ (Grassett and Murray 1967). The metal ion content in each protein was analyzed by flame atomic absorption spectrophotometry (WFX-110, BRAIC, Beijing, China).

Electrospray ionization mass spectrometry (ESI-MS) was used to determine the molecular weights of hGIF and its mutants. Each protein was dissolved in 1% formic acid (v/v) at a concentration of 10 ng $ml^{-1}$. The measurement was carried out on a Bruker Esquire 3000 electrospray ionization mass spectrometer (Bruker Daltonics, Bremen, Germany). The instrument conditions were listed as below: capillary volt, 4 kV; dry gas, 5 l $min^{-1}$; nebulizer gas, 15 PSI (pounds per square inch); infusion flow rate, 3 µl $min^{-1}$.

### Ultraviolet-visible and circular dichroism spectra

Ultraviolet-visible (UV-vis) absorption spectra were scanned from 200 to 300 nm on a HP8453 (Hewlett-Packard, Palo Alto, CA, USA) UV-vis spectrophotometer at room temperature using a 1.0 cm quartz cuvette. Circular dichroism (CD) spectra were measured in the range of 200–300 nm on a Jasco (Tokyo, Japan) J-715 spectropolarimeter at room temperature in 10 mM Tris–HCl, 100 mM KCl, pH 8.0.

### pH titration

pH titration was performed as follows: 6–7 μM $Cd^{2+}$-reconstituted proteins were dissolved in 10 mM Tris–HCl, 100 mM KCl, pH 8.0, then titrated with increasing amounts of 1 M HCl (Shaw et al. 1991). The pH was measured directly in the cuvette with a pH microelectrode (SCHOTT-16PH, Germany). The progress of acidification was recorded by UV-vis spectrophotometer. Apparent $Cd^{2+}$-binding constants at pH 7.0 of hGIF and its mutants were determined as described previously (Kagi and Vallee 1961; Shaw et al. 1991; Vasak and Kagi 1983; Wang et al. 1994). In all case, the p*K*a values of cysteine side chains were assumed to be equal to those of rabbit MT isoforms (p*K*a = 8.9) (Vasak and Kagi 1983).

### Reaction with DTNB

Reactions of $Cd^{2+}$-reconstituted hGIF and its mutants with DTNB were studied as described previously (Shaw et al. 1991): 3.5 μM protein reacted with 1 mM DTNB in 10 mM Tris–HCl, pH 8.0, containing 100 mM KCl at 25°C. The reaction was monitored at 412 nm ($\varepsilon_{412}$ = 13,600 $mol^{-1}$ $cm^{-1}$) on a HP8453 UV-vis spectrophotometer at 20 s intervals for 60 min.

### Preparation of rat brain extracts

Rat brain extracts were prepared as described previously (Chung et al. 2002b; Uchida et al. 1988). Briefly, the whole brain of adult male Hooded Wistar rat (~200 g) was removed and homogenized in one volume of Hanks buffer, followed by centrifugation at 100*g*. The supernatant was collected and filter-sterilized (0.22 μm filter, Millipore, Billerica, MA, USA). The total protein concentration of freshly prepared rat brain extracts was determined by the Bradford method (Bradford 1976). Extracts were used immediately at a total protein concentration of 150 μg $ml^{-1}$ (Chung et al. 2002b).

### Culture of cerebral cortical cells

Cultures of cerebral cortical cells were prepared as described previously with slight modifications (Chung et al. 2002b; Sewell et al. 1995). Briefly, cerebral cortices of Wistar rat fetuses (day 15) were removed and cells were dissociated mechanically by passing coarsely minced cortical tissues gently and repeatedly through a pipette. Tissue debris was removed by gently passing through a filter. Cells were washed and suspended in a specific culture medium developed for selective neuronal growth, consisting of Neurobasal-A medium (GIBCO), 0.1% (f/c) B-27 supplement (GIBCO), and 0.1 mM (f/c) L-glutamine (sigma). Then, cells were seeded on polylysine-coated 24- and 96-well culture plates at a density of $5 \times 10^5$ and $2 \times 10^6$ cells/ml, respectively. Cultures were maintained in a 37°C chamber under an atmosphere of humidified air containing 5% $CO_2$. Four hours later, the culture medium was replaced with fresh medium containing 150 μg $ml^{-1}$ rat brain extract and 10–20 μg $ml^{-1}$ proteins (Chung et al. 2002b). Cultures were maintained in the same conditions for 3 days.

### Calculations and analysis of neuron culture

To quantitatively analyze effect of hGIF and its mutants on initial neurite extension, cultures (24-well) were fixed in 4% paraformaldehyde and then stained with Trypan blue. Neurite length was obtained by measuring the distance between the end of the neurite and cell surface using the Leica Qwin program (Rueil Malmaison, France), and at least 60 neurons with more than 100 neurites were recorded in each individual experiment.

The percentage of neuron survival was determined by a MTT cell reduction assay (Cory et al. 1991). Briefly, 20 μl of MTT solution (5 mg $ml^{-1}$) in 0.02 M PBS was added to each well (96-well plate) and incubated at 37°C for 3 h. After incubation, unreacted dye and medium were removed, and 150 μl dimethyl sulfoxide (DMSO) was added to each well

to solubilize the MTT-formazan product formed. Then, the MTT-formazan products were quantified by measuring the absorbance at 490 nm using a Bio-Rad 680 Multireader (California, USA), and background readings of MTT incubated in cell-free medium were subtracted from each value before calculations.

## Results and discussion

After expression and purification, the yield of each mutant protein was about 8 ~ 9 mg per liter culture. Their molecular masses were determined by ESI-MS and were in good agreement with the theoretical values (Table 1). The metal contents of hGIF and its variants were obtained by flame atomic absorption spectrophotometer (Table 1). It was demonstrated that $Cd^{2+}$ is a useful probe for $Zn^{2+}$ binding sites in MTs, providing a wealth of structural information on $Zn^{2+}$-substituted MTs (Vasak 1998). Furthermore, $Cd^{2+}$-substituted MTs show a number of advantages over $Zn^{2+}$-substituted MTs, including a tendency toward higher oxidation stability, a pronounced and thus easier to detect and quantify LMCT band, as well as the use of the $^{111}Cd$ or $^{113}Cd$ isotopes for NMR experiments, etc. Thus, $Cd^{2+}$ was frequently used as a substitute of $Zn^{2+}$ for structural studies of hGIF (Cai et al. 2006; Hasler et al. 2000; Romero-Isart et al. 2002). In the present studies, $Cd^{2+}$-substituted MTs were adopted in both spectroscopic and metal-binding studies while $Zn^{2+}$-substituted MTs were only used in bioassay because $Cd^{2+}$-MT is cytotoxic to neurons (Sewell et al. 1995).

**Table 1** Mass spectrometry results and metal contents of hGIF and its mutants

| Protein | Mr (calc.)[a] (Da) | Mr (meas.)[b] (Da) | Metal contents |
|---|---|---|---|
| hGIF | 7,071 | 7,070.7 | 7 ± 0.3 |
| K31/32A | 6,957 | 6,956.8 | 7 ± 0.2 |
| K31/32E | 7,073 | 7,072.7 | 7 ± 0.4 |
| KKS-SP | 6,912 | 6,910.0 | 7 ± 0.2 |

[a] The theoretical molecular mass

[b] The measured molecular mass

Figure 2a shows the UV-vis spectra of $Cd_7$-hGIF and its mutants. All the spectra maintained similar shape and showed absorption shoulders around 250 nm, characteristic of Cd–S ligand-to-metal charge transfer (LMCT) (Vasak et al. 1981). There was no absorption around 280 nm due to the absence of aromatic amino acid residue.

Circular dichroism spectroscopy is commonly adopted to investigate the metal–thiolate cluster geometry and secondary structures of the enfolding polypeptide chains of MTs (Cai et al. 2006; Faller and Vasak 1997; Hasler et al. 1998; Kagi and Schaffer 1988; Romero-Isart et al. 2002; Stillman et al. 1987). Figure 2b shows the CD spectra of $Cd_7$-hGIF and its mutants in the range of 200–300 nm. The CD spectrum of hGIF nicely matched the results

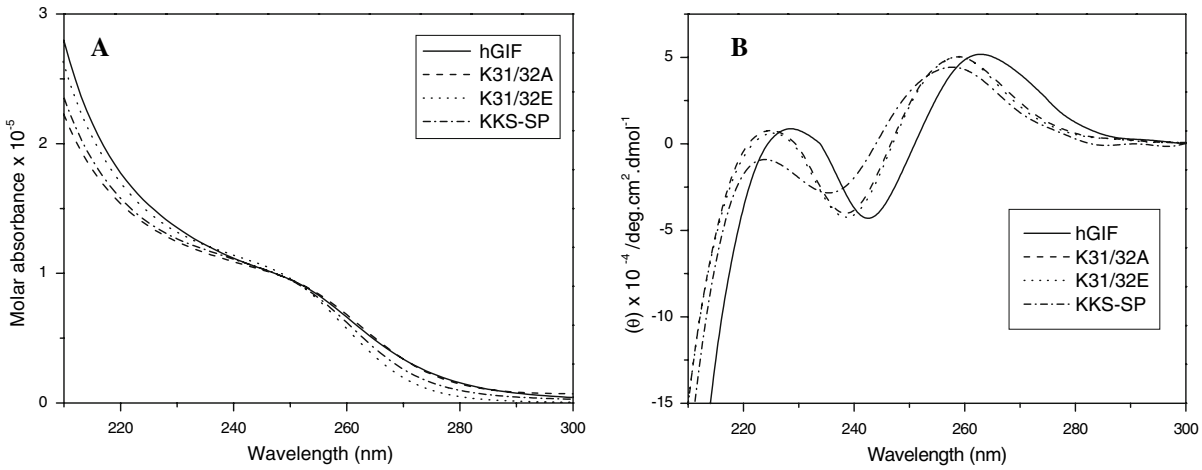


**Fig. 2** UV (**a**) and CD (**b**) spectra of $Cd_7$-hGIF, the K31/32A mutant, the K31/32E mutant and the KKS-SP mutant. All proteins are dissolved in 10 mM Tris–HCl, 100 mM KCl, pH 8.0

from previous reports (Hasler et al. 1998, 2000) and showed bands at 259 (+), 239 (−) and 225 (+) nm. The bands around 260 (+) and 240 nm (−) are the contributions from Cd–thiolate clusters and the band around 225 nm (+) has been assigned to the interaction between the Cd–thiolate clusters and the peptide wrapping around (Stillman et al. 1987). The CD spectra of the K31/32A and K31/32E mutants were almost the same as that of hGIF, indicating that change of the positive charge of lysine residues did not affect the overall structure and metal–thiolate cluster geometry apparently. However, compared to hGIF, the CD profile of the KKS-SP mutant was blue shifted, which undoubtedly suggested alterations of the cluster geometry and conformation of enfolded polypeptide in this mutant. It was demonstrated that the two domains in metallothionein do not work independently and domain–domain interactions do exist in MT and affect the structure and function of each domain (Ding et al. 2007; Jiang et al. 2000; Zangger and Armitage 2002). In the KKS-SP mutant, introduction of a rigid proline residue in the short linker region may alter the relative orientation of the two domains and changed the domain–domain interaction of hGIF to some extent, thus impacting the metal–thiolate geometry and polypeptide structure.

Ultraviolet absorbance at 250 nm was recorded during pH titration in order to investigate the stability of the Cd–thiolate clusters (Fig. 3). Displacement of $Cd^{2+}$ from MTs with increasing concentrations of proton was followed by a decrease in the Cd–S LMCT absorption band at 250 nm. According to previous studies, pH titration curves of MTs are usually divided into two stages reflecting different stabilities of the two metal–thiolate clusters and the metal–thiolate cluster in the $\beta$-domain is more easily dissociated (Cismowski and Huang 1991). Stabilities of the Cd–thiolate clusters were quantitatively studied by calculating their apparent Cd-binding constants at pH 7.0, which could be easily estimated from the midpoint values of pH titration curves (Kagi and Vallee 1961; Shaw et al. 1991; Vasak and Kagi 1983; Wang et al. 1994). Compared with hGIF, the stabilities of the $Cd_3S_9$ cluster in the $\beta$-domain of the mutant proteins significantly decreased (Table 2). This result undoubtedly reflected that the linker $^{31}$KKS$^{33}$ was more helpful in maintaining the stability of the metal–thiolate in the $\beta$-domain of hGIF. Recently, we predicted the structure of hGIF by

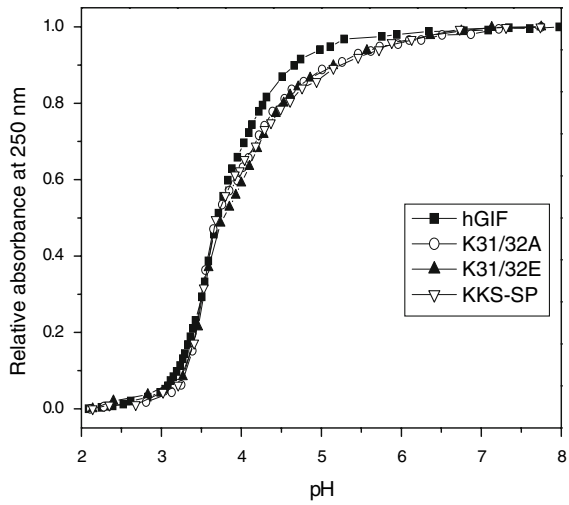


**Fig. 3** UV absorbance at 250 nm versus pH during pH titration of $Cd_7$-hGIF (*solid squares*), the K31/32A mutant (*open circles*), the K31/32E mutant (*solid triangles*) and the KKS-SP mutant (*open triangles*). All proteins are dissolved in 10 mM Tris–HCl, 100 mM KCl, pH 8.0

molecular dynamics simulation and found Lys32 in the linker formed a hydrogen bond with Cys22 (2.92 Å) in the $\beta$-domain [Our unpublished data]. Interestingly, the same hydrogen bond between Lys31 (according to Lys32 in hGIF) and Cys21 (according to Cys22 in hGIF) is also observed in the X-ray structure of rat liver MT2. This hydrogen bond is believed to play an important role in the stability of metal–thiolate cluster in the $\beta$-domain of MT2 (Braun et al. 1992; Robbins et al. 1991). Hence, when we changed the KKS to other sequence, the hydrogen bond between Lys32 and Cys22 might vanish, thus decreased the stability of the metal–thiolate clusters in the $\beta$-domain of hGIF.

The reaction of metallothionein with DTNB is used to estimate the solvent accessibility of the metal–thiolate clusters and usually exhibits biphasic kinetics (Shaw et al. 1991). In the case of hGIF, the fast and slow phase correspond to the reaction of DTNB with the $\beta$-domain and $\alpha$-domain, respectively (Sewell et al. 1995). Observed rate constants were obtained by plotting $\ln(A_\infty - A_t)$ versus time and these constants were listed in Table 3. The fast reaction rate constants ($k_f$) of the three mutants were similar and were about twice that of hGIF, showing that the solvent accessibilities of the $Cd_3S_9$ clusters in the three mutants were greatly enhanced. By contrast, the slow reaction rate constants ($k_s$) of the three

**Table 2** Apparent Cd-binding constants of hGIF and its mutants

| Protein | Midpoint ($Cd_3S_9$) | $K_{Cd,app}$ ($M^{-1}$) of the $\beta$-domain ($\times 10^{13}$) | Midpoint ($Cd_4S_{11}$) | $K_{Cd,app}$ ($M^{-1}$) of the $\alpha$-domain ($\times 10^{15}$) |
|---|---|---|---|---|
| hGIF | 4.08 | 7.68 | 3.31 | 1.32 |
| K31/32A | 4.37 | 1.30 | 3.33 | 1.44 |
| K31/32E | 4.29 | 1.03 | 3.36 | 1.02 |
| KKS-SP | 4.39 | 0.91 | 3.35 | 1.09 |

Apparent Cd-binding constants ($K_{Cd,\ app}$) were determined by the competition between metal ions and protons for the thiolate ligands and extrapolated to pH 7.0. For details, please see "Materials and methods"

**Table 3** Observed rate constants for the reaction of DTNB with hGIF and its mutants

| Protein | $k_f$* ($\times 10^{-3}$ $s^{-1}$) | $k_s$* ($\times 10^{-4}$ $s^{-1}$) |
|---|---|---|
| hGIF | 2.5 ± 0.1 | 9.3 ± 0.2 |
| K31/32A | 4.2 ± 0.1 | 8.6 ± 0.1 |
| K31/32E | 4.3 ± 0.1 | 7.5 ± 0.2 |
| KKS-SP | 4.3 ± 0.1 | 8.5 ± 0.2 |

$k_f$ is the rate constant for the fast reaction, $k_s$ is the rate constant for the slow reaction

mutants were similar to that of hGIF, indicating the solvent accessibilities of the $Cd_4S_{11}$ clusters in the three mutants did not change much.

Figure 4 shows the effect of the hMT1g (negative control), hGIF (positive control) and its mutants on neuron survival determined by a MTT cell reduction assay. MTT is reduced to blue formazan by mitochondrial dehydrogenase of living cells but not by dead cells (Cory et al. 1991). Apparently, hGIF revealed the neuronal growth inhibitory activity, which was not shared by hMT1g. This result agreed well with those reported previously (Chung et al. 2002b; Hasler et al. 2000; Sewell et al. 1995). Compared to hGIF, the K31/32A and K31/32E mutants exhibited similar but significantly reduced bioactivity, while the KKS-SP mutant lost bioactivity completely. Hence, we concluded that the conserved liker KKS played important roles in the bioactivity of hGIF.

Effect of hGIF and its mutants on neurite extension was also studied (Fig. 5). The average neurite length of neurons treated by hMT1g, hGIF, the K31/32A mutant, the K31/32E mutant and the KKS-SP mutant were 164 ± 4, 85 ± 3, 115 ± 3, 127 ± 5 and 159 ± 4 μm, respectively. This result paralleled well with the data of neuron survival mentioned above.

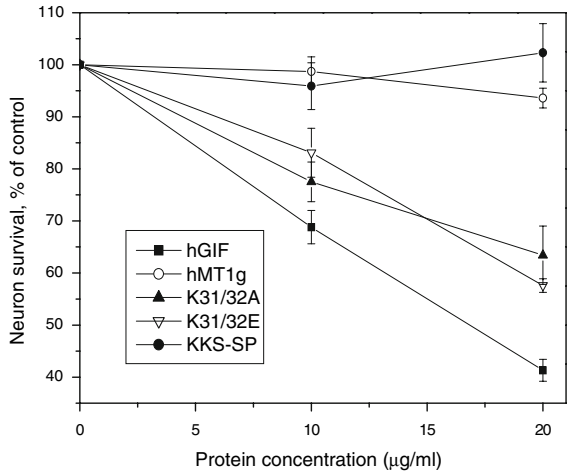


**Fig. 4** Effect of $Zn_7$-hGIF (*solid squares*), the K31/32A mutant (*solid triangles*), the K31/32E mutant (*open triangles*) and the KKS-SP mutant (*solid circles*) on survival of cortical neurons cultured in the presence of adult rat brain extract (150 μg/ml) after 3 days, determined by a MTT cell reduction assays. As a comparison, result of hMT1g (*open circles*) under the same conditions was also shown. *Error bars* represent standard error values

The neuronal growth inhibitory activity of hGIF is unique in MT family (Palmiter et al. 1992; Uchida et al. 1991; Uchida and Tomonaga 1989). More and more evidences revealed that the bioactivity of hGIF mainly relates to the essential metal release (Erickson et al. 1997; Palmiter 1995) and its characteristic conformation (Ni et al. 2007; Sewell et al. 1995), especially the $\beta$-domain. The metal-releasing ability, determined by the stability and solvent accessibility of the metal–thiolate cluster in the $\beta$-domain of hGIF, is exquisitely modulated by domain–domain interaction and protein's conformation (Ding et al. 2008, 2007; Faller et al. 1999; Ni et al. 2007). Furthermore, the characteristic conformation of hGIF is also

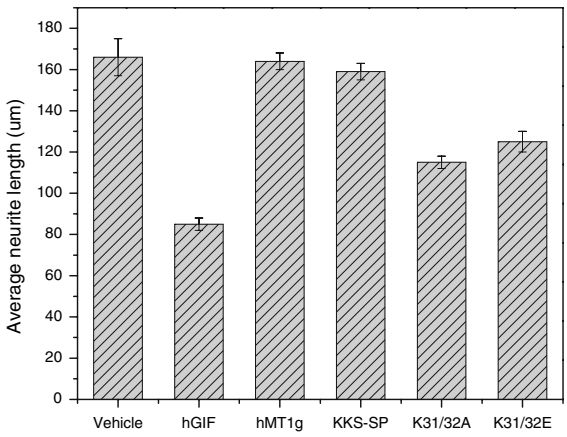


**Fig. 5** Effect of $Zn_7$-hGIF, the K31/32A mutant, the K31/32E mutant and the KKS-SP mutant on neurite extension in the presence of adult rat brain extract (150 μg/ml) after 3 days, determined by average neurite length of 60 neurons. As a comparison, result of hMT1g (negative control) and 0.1% PBS (vehicle) under the same conditions was also shown. *Error bars* represent standard error values

suggested to provide an interface for the interaction with its partner protein (Ni et al. 2007; Sewell et al. 1995). In the present study, it was found that both the K31/32A and K31/32E mutants showed reduced bioactivity. Based on the results of biochemical studies, the overall structure of the two mutants did not change much, but the stability and solvent accessibility of the $Cd_3S_9$ clusters of the two mutants altered much. Thereby, the reductions in bioactivity of the two mutants were most likely due to the change in the stability and solvent accessibility in the $Cd_3S_9$ cluster. Interestingly, the bioactivity of the KKS-SP mutant was completely abolished although the stability and solvent accessibility of the KKS-SP mutant were similar to those of the K31/32A and K31/32E mutants. However, it should be noted that mutating KKS to SP not only changed the stability and solvent accessibility of metal–thiolate cluster in the $\beta$-domain, but more significantly altered the domain–domain interactions/relative orientation of the two domains of hGIF, thus making the KKS-SP mutant lose its bioactivity completely.

## Conclusions

It has been demonstrated that the two domains of hGIF do not work independently (Faller et al. 1999) and domain–domain interactions do exist in hGIF and affect the function of each domain in our previous studies (Ding et al. 2008, 2007). However, the definite mechanism of domain–domain interactions has not been established due to lack of crystal structure of hGIF and potential contributors modulating the inter-domain interactions of hGIF remain unknown. Our previous mutational study indicated that deletion of the EAAEAE insert near the C-terminus (the Δ55-60 mutant), which is unrestricted and presents highly dynamic conformation and flexible loop in NMR structure (Wang et al. 2006), makes the $\beta$-domain more compact and greatly increases the stability of the metal–thiolate cluster in the $\beta$-domain toward DTNB and S-nitrosocysteine (Zheng et al. 2003). Interestingly, bioassay results showed that the Δ55-60 mutant displayed significantly reduced bioactivity [Our unpublished data]. Hence, we conclude that the EAAEAE insert modulates the domain–domain interactions in hGIF, and deletion of the EAAEAE insert makes the $\beta$-domain more stable, thus affecting its bioactivity. In the present study, by study of a series of artificial mutants at linker region of hGIF we provided solid evidences revealing that the native KKS linker also played important roles in regulating the domain–domain interactions of hGIF and modulated the properties (including the stability and the solvent accessibility) of the $Cd_3S_9$ cluster in the $\beta$-domain and the conformation, thus playing important roles in the biological activity of hGIF. We believe that these results shall extend our knowledge of hGIF and provide us more information to understand the molecular mechanism of the bioactivity of this fascinating molecule.

**Acknowledgments** The authors are grateful to the financial support of the National Natural Science Foundation of China (Grant 29281005). We appreciate Professor J. H. R. Kägi from Department of Biochemistry of the University of Zürich for helpful discussion and valuable advice.

## References

Adlard PA, Bush AI (2006) Metals and Alzheimer's disease. J Alzheimers Dis 10:145–163

Bradford MM (1976) Rapid and sensitive method for quantitation of microgram quantities of protein utilizing principle of protein dye binding. Anal Biochem 72:248–254. doi:10.1016/0003-2697(76)90527-3

Braun W, Vasak M, Robbins AH et al (1992) Comparison of the NMR solution structure and the X-ray crystal structure of rat metallothionein-2. Proc Natl Acad Sci USA 89: 10124–10128. doi:10.1073/pnas.89.21.10124

Brown DR, Kozlowski H (2004) Biological inorganic and bioinorganic chemistry of neurodegeneration based on prion and Alzheimer diseases. Dalton Trans:1907–1917

Cai L, Li XK, Song Y et al (2005) Essentiality, toxicology and chelation therapy of zinc and copper. Curr Med Chem 12:2753–2763. doi:10.2174/092986705774462950

Cai B, Zheng Q, Teng XC et al (2006) The role of Thr5 in human neuron growth inhibitory factor. J Biol Inorg Chem 11:476–482. doi:10.1007/s00775-006-0097-6

Chung RS, Holloway AF, Eckhardt BL et al (2002a) Sheep have an unusual variant of the brain-specific metallothionein, metallothionein-III. Biochem J 365:323–328. doi: 10.1042/BJ20011751

Chung RS, Vickers JC, Chuah MI et al (2002b) Metallothionein-III inhibits initial neurite formation in developing neurons as well as postinjury, regenerative neurite sprouting. Exp Neurol 178:1–12. doi:10.1006/exnr.2002.8017

Cismowski MJ, Huang PC (1991) Effect of cysteine replacements at position-13 and position-50 on metallothionein structure. Biochemistry 30:6626–6632. doi:10.1021/bi00240a036

Cory AH, Owen TC, Barltrop JA et al (1991) Use of an aqueous soluble tetrazolium formazan assay for cell growth assays in culture. Cancer Commun 3:207–212

Ding ZC, Zheng Q, Cai B et al (2007) Effect of α-domain substitution on the structure, property and function of human neuronal growth inhibitory factor. J Biol Inorg Chem 12: 1173–1179. doi:10.1007/s00775-007-0287-x

Ding ZC, Zheng Q, Cai B et al (2008) Study on structure-property-reactivity-function relationship of human neuronal growth inhibitory factor (hGIF). J Inorg Biochem 102: 1965–1972. doi:10.1016/j.jinorgbio.2008.07.007

Erickson JC, Hollopeter G, Thomas SA et al (1997) Disruption of the metallothionein-III gene in mice: analysis of brain zinc, behavior, and neuron vulnerability to metals, aging, and seizures. J Neurosci 17:1271–1281

Faller P, Vasak M (1997) Distinct metal–thiolate clusters in the N-terminal domain of neuronal growth inhibitory factor. Biochemistry 36:13341–13348. doi:10.1021/bi9711994

Faller P, Hasler DW, Zerbe O et al (1999) Evidence for a dynamic structure of human neuronal growth inhibitory factor and for major rearrangements of its metal–thiolate clusters. Biochemistry 38:10158–10167. doi:10.1021/bi990489c

Grassett DR, Murray JF (1967) Determination of sulfhydryl groups with 2,2′- or 4,4′-dithiodipyridine. Arch Biochem Biophys 119:41–49. doi:10.1016/0003-9861(67)90426-2

Hasler DW, Faller P, Vasak M (1998) Metal–thiolate clusters in the C-terminal domain of human neuronal growth inhibitory factor (GIF). Biochemistry 37:14966–14973. doi:10.1021/bi9813734

Hasler DW, Jensen LT, Zerbe O et al (2000) Effect of the two conserved prolines of human growth inhibitory factor (metallothionein-3) on its biological activity and structure fluctuation: comparison with a mutant protein. Biochemistry 39:14567–14575. doi:10.1021/bi001569f

Jiang LJ, Vasak M, Vallee BL et al (2000) Zinc transfer potentials of the α- and β-clusters of metallothionein are affected by domain interactions in the whole molecule. Proc Natl Acad Sci USA 97:2503–2508. doi:10.1073/pnas.97.6.2503

Kagi JHR, Schaffer A (1988) Biochemistry of metallothionein. Biochemistry 27:8509–8515. doi:10.1021/bi00423a001

Kagi JHR, Vallee BL (1961) Metallothionein—cadmium-containing and zinc-containing protein from equine renal cortex. II. physicochemical properties. J Biol Chem 236: 2435–2442

Kobayashi H, Uchida Y, Ihara Y et al (1993) Molecular cloning of rat growth inhibitory factor cDNA and the expression in the central nervous system. Brain Res Mol Brain Res 19: 188–194. doi:10.1016/0169-328X(93)90025-K

Margoshes M, Vallee BL (1957) A cadmium protein from equine kidney cortex. J Am Chem Soc 79:4813–4814. doi: 10.1021/ja01574a064

Narula SS, Brouwer M, Hua Y et al (1995) Three-dimensional solution structure of *Callinectes sapidus* metallothionein-1 determined by homonuclear and heteronuclear magnetic resonance spectroscopy. Biochemistry 34:620–631. doi: 10.1021/bi00002a029

Ni FY, Cai B, Ding ZC et al (2007) Structural prediction of the β-domain of metallothionein-3 by molecular dynamics simulation. Proteins-Struct Funct Bioinform 68:255–266. doi:10.1002/prot.21404

Oz G, Zangger K, Armitage IM (2001) Three-dimensional structure and dynamics of a brain specific growth inhibitory factor: metallothionein-3. Biochemistry 40:11433–11441. doi:10.1021/bi010827l

Palmiter RD (1995) Constitutive expression of metallothionein-III (MT-III), but not MT-I, ihibits growth when cells become zinc-deficient. Toxicol Appl Pharmacol 135:139–146. doi:10.1006/taap.1995.1216

Palmiter RD, Findley SD, Whitmore TE et al (1992) MT-III, a brain-specific member of the metallothionein gene family. Proc Natl Acad Sci USA 89:6333–6337. doi:10.1073/pnas.89.14.6333

Pountney DL, Fundel SM, Faller P et al (1994) Isolation, primary structures and metal binding properties of neuronal growth inhibitory factor (GIF) from bovine and equine brain. FEBS Lett 345:193–197. doi:10.1016/0014-5793(94)00452-8

Rasia RM, Bertoncini CW, Marsh D et al (2005) Structural characterization of copper(II) binding to α-synuclein: insights into the bioinorganic chemistry of Parkinson's disease. Proc Natl Acad Sci USA 102:4294–4299. doi: 10.1073/pnas.0407881102

Robbins AH, McRee DE, Williamson M et al (1991) Refined crystal structure of Cd, Zn metallothionein at 2.0 A resolution. J Mol Biol 221:1269–1293

Romero-Isart N, Jensen LT, Zerbe O et al (2002) Engineering of metallothionein-3 neuroinhibitory activity into the inactive isoform metallothionein-1. J Biol Chem 277: 37023–37028. doi:10.1074/jbc.M205730200

Sewell AK, Jensen LT, Erickson JC et al (1995) Bioactivity of metallothionein-3 correlates with its novel β-domain sequence rather than metal-binding properties. Biochemistry 34:4740–4747. doi:10.1021/bi00014a031

Shaw CF, Savas MM, Petering DH (1991) Ligand substitution and sulfhydryl reactivity of metallothionein. Methods Enzymol 205:401–414. doi:10.1016/0076-6879(91)05122-C

Stillman MJ, Cai W, Zelazowski AJ (1987) Cadmium binding to metallothioneins-domain specificity in reactions of

α-fragment and β-fragment, apometallothionein, and zinc metallothionein with $Cd^{2+}$. J Biol Chem 262:4538–4548

Uchida Y, Tomonaga M (1989) Neurotrophic action of Alzheimer's disease brain extract is due to the loss of inhibitory factors for survival and neurite formation of cerebral cortical neurons. Brain Res 481:190–193. doi:10.1016/0006-8993(89)90503-9

Uchida Y, Ihara Y, Tomonaga M (1988) Alzheimer's disease brain extract stimulates the survival of cerebral cortical neurons from neonatal rats. Biochem Biophys Res Commun 150:1263–1267. doi:10.1016/0006-291X(88)90765-6

Uchida Y, Takio K, Titani K et al (1991) The growth inhibitory factor that is deficient in the Alzheimer's disease brain is a 68 amino acid metallothionein-like protein. Neuron 7:337–347. doi:10.1016/0896-6273(91)90272-2

Vasak M (1991) Standard isolation procedure for metallothionein. Methods Enzymol 205:41–44. doi:10.1016/0076-6879(91)05082-7

Vasak M (1998) Application of Cd-113 NMR to metallothioneins. Biodegradation 9:501–512. doi:10.1023/A:1008346231847

Vasak M, Kagi JH (1983) Metal ions in biological system. Marcel Dekker Inc., New York and Basel

Vasak M, Kagi JHR, Hill HAO (1981) Zinc(II), cadmium(II), and mercury(II) thiolate transitions in metallothionein. Biochemistry 20:2852–2856. doi:10.1021/bi00513a022

Wang YJ, Mackay EA, Kurasaki M et al (1994) Purification and characterization of recombinant sea-urchin metallothionein expressed in *Escherichia coli*. Eur J Biochem 225:449–457. doi:10.1111/j.1432-1033.1994.00449.x

Wang H, Zhang Q, Cai B et al (2006) Solution structure and dynamics of human metallothionein-3 (MT-3). FEBS Lett 580:795–800. doi:10.1016/j.febslet.2005.12.099

Williamson MP (1994) The structure and function of proline-rich regions in proteins. Biochem J 297:249–260

Yu WH, Cai B, Gao Y et al (2002) Expression, characterization, and reaction of recombinant monkey metallothionein-1 and its C33M mutant. J Protein Chem 21:177–185. doi:10.1023/A:1015324717115

Zangger K, Armitage IM (2002) Dynamics of interdomain and intermolecular interactions in mammalian metallothioneins. J Inorg Biochem 88:135–143. doi:10.1016/S0162-0134(01)00379-8

Zheng Q, Cai B, Chen D et al (2003) The reaction of metallothionein-3 with DTNB. Chem Lett 32:616–617. doi:10.1246/cl.2003.616